Measurement of Spin Effects in $p_\uparrow + p_\uparrow \rightarrow p + p$ at 18.5 GeV/c

D. G. Crabb, I. Gialas, A. D. Krisch, A. M. T. Lin, D. C. Peaslee, R. A. Phelps, R. S. Raymond, T. Roser, J. A. Stewart, and K. M. Terwilliger

Randall Laboratory of Physics, The University of Michigan, Ann Arbor, Michigan 48109

K. A. Brown, G. T. Danby, F. Z. Khiari, and L. G. Ratner

Alternating Gradient Synchrotron Department, Brookhaven National Laboratory, Upton, New York 11973

J. R. O'Fallon

Division of High Energy Physics, U. S. Department of Energy, Washington, D.C. 20545

and

G. Glass

Department of Physics, Texas A&M University, College Station, Texas 77843

(Received 16 March 1988)

We measured the analyzing power A and the spin-spin correlation parameter A_{nn} in medium-$P_\perp^2$ proton-proton elastic scattering, using a polarized-proton target and the 18.5-GeV/c Brookhaven Alternating-Gradient Synchrotron polarized-proton beam. We found sharp dips in both A and A_{nn}, which occur at different $P_\perp^2$ values. The unexpected sharp structure in the spin-spin force occurs near $P_\perp^2 = 2.3$ (GeV/c)^2 where the elastic cross section has no apparent structure.

PACS numbers: 13.85.Dz, 13.88.+e

Spin effects in high-energy strong interactions can be studied with polarized-proton beams and polarized-proton targets. Experiments with the Argonne Zero-Gradient Synchrotron polarized-proton beam found a large and unexpected spin-spin correlation parameter A_{nn} in high-$P_\perp^2$ proton-proton elastic scattering.[1,2] Recent Brookhaven Alternating Gradient Synchrotron (AGS) experiments[3] found a large analyzing power A in $p+p_\uparrow \rightarrow p+p$ at 28 GeV/c in the large-$P_\perp^2$ region near 6.5 (GeV/c)^2. In 1984 a high-energy polarized-proton beam was accelerated at the AGS and we measured A_{nn} with limited precision.[4,5] The energy, intensity, reliability, and polarization of the AGS polarized beam have now increased significantly. This allowed us to study spin effects in p-p elastic scattering at $P_{\rm lab} = 18.5$ GeV/c with good precision. We found that both A and A_{nn} appear to change rapidly with $P_\perp^2$; both exhibit a sharp dip but at somewhat different $P_\perp^2$ values.

The experiment was run at the AGS with an accelerated polarized-proton beam of about 2×10^{10} protons per pulse at 18.5 GeV/c, with an average polarization of (43 ± 3)%. The AGS reached a maximum polarization of about 52% at 18.5 GeV/c with a peak accelerated intensity of about 2.5×10^{10} protons per pulse. The acceleration of polarized protons in the AGS has been described in earlier publications.[4-7]

The high-energy polarimeter shown in Fig. 1 measured the beam polarization by observing the left-right asymmetry in proton-proton elastic scattering at $P_\perp^2 = 0.3$ (GeV/c)^2, where A was taken[7] to be (3.9 ± 0.3)%. The vertical bends in our extracted beam line caused a polarization loss of about 2%, giving an average beam polar-

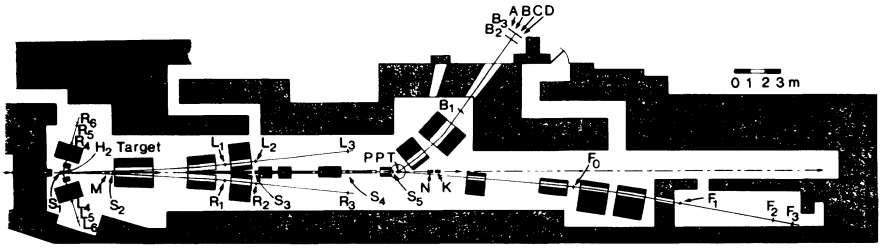

FIG. 1. Layout of the experiment. The high-energy polarimeter on the left used a liquid-hydrogen target to measure the left-right asymmetry in p-p elastic scattering. The polarized proton beam then scattered in the vertically polarized proton target and the elastic events were detected by the spectrometer which contained magnets for momentum analysis and the F and B scintillation-counter hodoscopes. The counters M, N, and K were intensity monitors, while the segmented wire ion chambers S_1, S_2, S_4, and S_5 monitored the beam's position, size, and angle.

ization for our data run of $(41 \pm 3)\%$; our average intensity was about 1.2×10^{10} polarized protons every 2.4 s. We scattered the polarized protons from the Michigan polarized-proton target (PPT) in our extracted beam line as shown in Fig. 1. The beam position and the 13×13-mm^2 FWHM ($H\times V$) beam size at our PPT were monitored continuously by four segmented wire ion chambers S_1, S_2, S_4, and S_5. Upstream steering magnets were servocoupled to split segmented wire ion chambers to reduce the horizontal beam motion; the average beam position was kept centered to within ±0.1 mm. The relative beam intensity was measured with an ion chamber (Ion), a secondary-emission chamber (SEC), and four scintillation-counter telescopes M, N, K, and B, which counted the secondary particles produced by the beam.

The Michigan PPT used the dynamic-nuclear-polarization technique at a magnetic field of 2.5 T and a temperature of 0.5 K produced by a ^{3}He-^{4}He-mixture evaporation cryostat.[8] For the target material we used ammonia (NH_3) with radiation-induced[9] unpaired electrons or ethyl amine borane ammonia (EABA) with chemically induced unpaired electrons. The 2-mm-diam beads of either NH_3 or EABA each had a free proton density of about 0.1 g/cm^3 and were contained in a cylindrical copper cavity 29 mm diam by 40 mm long. The 2.5-T field (B) and the 0.5-K temperature (T) polarized the unpaired electrons in the beads. Microwaves of about 70 GHz were used to transfer the electron polarization to the free hydrogen protons in the beads. The proton polarization was reversed by our changing the microwave frequency by about 0.37 GHz.

We continuously monitored radial variations in the target polarization P_T, using a 106.8-MHz NMR system with two independent coils of different radii. These coils were calibrated in special runs with the microwaves and the beam both turned off; the thermal-equilibrium proton polarization was then given by the Boltzmann distribution

$$P_{TE}=\tanh(\mu_p B/kT). \tag{1}$$

There was a $\pm3\%$ relative uncertainty in P_{TE}, and thus in P_T, caused mostly by the temperature uncertainty. The average target polarization was about 65% for the EABA beads and about 44% for the more radiation-resistant NH_3 beads.

Elastic-scattering events were detected by the double-arm spectrometer FB shown in Fig. 1. The angles and momenta of both outgoing protons were measured with six magnets and the forward and backward eight-channel scintillation counter hodoscopes. A p-p elastic-scattering event was defined by a sevenfold FB coincidence between the appropriate channels of the $F=F_0F_1F_2F_3$ arm and the $B=B_1B_2B_3$ arm. The four (25×35 cm^2) B_3 counters and the four (7.5×14 cm^2) F_3 counters along with the vertically split F_2 and B_2 counters defined eight channels, each with a center-of-mass solid angle of about 3×10^{-4} sr. The other counters were overmatched to allow for beam size and divergence, magnet variations, and multiple Coulomb scattering. The momentum bite $\Delta P/P$ was about 5%. Accidental coincidences were continuously monitored by several delayed FB coincidence circuits. The data at each $P_\perp^2$ point were corrected with the measured accidental rate of about 0.1%.

At each spectrometer magnet setting we simultaneously measured two different $P_\perp^2$ points which each covered a $P_\perp^2$ range of about 0.3 $(\mathrm{GeV}/c)^2$. We varied the coincidence-logic timing and the magnet currents about the calculated values to assure that we had a clean elastic signal at the correct $P_\perp^2$ value. The background rate for nonhydrogen events was measured by our replacing the normal PPT beads with Teflon (CF_2) beads which contain no hydrogen. We multiplied the raw A and A_{nn} data by the measured nonhydrogen-background correction factors of 1.05 ± 0.005 at the smallest-$P_\perp^2$ points and 1.07 ± 0.01 at the largest-$P_\perp^2$ points; we used the interpolated value of 1.06 ± 0.01 for the points in between.

The vertically polarized proton beam was scattered from the vertically polarized proton target and we detected elastic events in the horizontal plane for each transverse beam spin state [$i=\uparrow$ or $\downarrow$ (up or down)] and each transverse target spin state ($j=\uparrow$ or $\downarrow$). We then obtained the normalized event rates $N(ij)$ by measuring the quantities

$$N(ij)=\mathrm{events}(ij)/I(ij). \tag{2}$$

For each (beam $=i$, target $=j$) spin state, events(ij) was the number of FB elastic events corrected for accidentals and nonhydrogen background, and $I(ij)$ was the relative beam intensity obtained by our averaging the monitors M, N, K, B, SEC, and Ion. The spin-spin correlation parameter A_{nn} and the analyzing power A were obtained from our measured $N(ij)$ by the equations

$$\begin{aligned}
A_{nn}&=\frac{1}{P_BP_T}\left[\frac{N(\uparrow\uparrow)-N(\uparrow\downarrow)-N(\downarrow\uparrow)+N(\downarrow\downarrow)}{N(\uparrow\uparrow)+N(\uparrow\downarrow)+N(\downarrow\uparrow)+N(\downarrow\downarrow)}\right],\\
A_B&=-\frac{1}{P_B}\left[\frac{N(\uparrow\uparrow)+N(\uparrow\downarrow)-N(\downarrow\uparrow)-N(\downarrow\downarrow)}{N(\uparrow\uparrow)+N(\uparrow\downarrow)+N(\downarrow\uparrow)+N(\downarrow\downarrow)}\right],\\
A_T&=-\frac{1}{P_T}\left[\frac{N(\uparrow\uparrow)-N(\uparrow\downarrow)+N(\downarrow\uparrow)-N(\downarrow\downarrow)}{N(\uparrow\uparrow)+N(\uparrow\downarrow)+N(\downarrow\uparrow)+N(\downarrow\downarrow)}\right],
\end{aligned} \tag{3}$$

where P_B and P_T are respectively the beam and target polarizations. The minus signs occur because our forward protons scattered to the right, which is opposite to the Ann Arbor convention.

Our results for proton-proton elastic scattering are plotted in Fig. 2 and listed in Table I along with our estimated uncertainty, which includes both statistical and systematic errors. A is the weighted average of A_B and A_T. For each datum point we had about 10^5 beam-spin

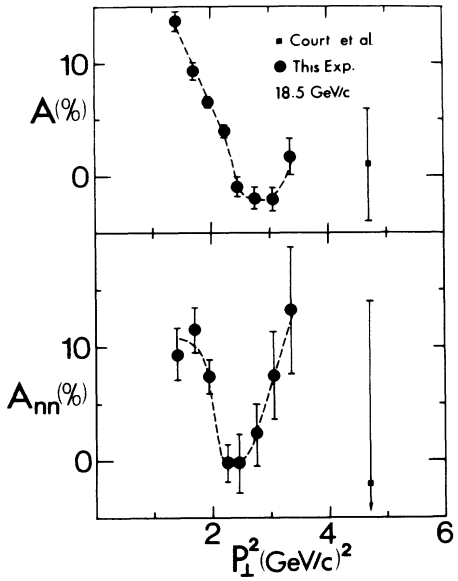

FIG. 2. Plot of the analyzing power A and the spin-spin correlation parameter A_{nn} as functions of momentum transfer squared for proton-proton elastic scattering at 18.5 GeV/c. The error bars include both statistical and systematic errors. The dashed lines are hand-drawn curves to guide the eye.

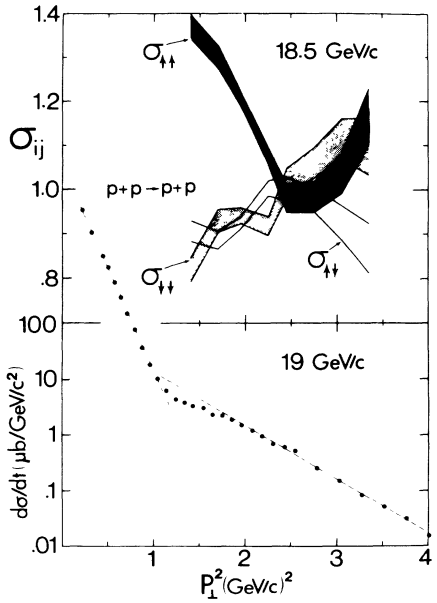

FIG. 3. The relative pure-initial-spin-state cross sections $\sigma_{\uparrow\uparrow}$, $\sigma_{\downarrow\downarrow}$, and $\sigma_{\uparrow\downarrow}\equiv[d\sigma(\uparrow\downarrow)/dt]\langle d\sigma/dt\rangle^{-1}$ plotted against $P_\perp^2$ for $p_\uparrow+p_\uparrow\rightarrow p+p$ at 18.5 GeV/c. The errors are given by the width of each band. The spin-averaged cross-section data of Allaby *et al.* (Ref. 28) at 19 GeV/c are also plotted for comparison. The dashed lines are exponentials in $P_\perp^2$.

reversals, which reduced the systematic errors in A_B and A_{nn} so that their average χ's were 0.93 and 1.03, respectively. However, we had only 12 to 30 target-spin reversals; thus A_T had χ's of 2.00 and 2.03 for the two small-$P_\perp^2$ points and we multiplied the statistical errors in A_T by these factors. For the other six points the average χ of A_T was 1.21 and we used the measured statistical error. Note that A_B and A_T, which were respectively measurements of A with the polarized beam and with the polarized target, were generally equal within our errors. This provided a good determination of our systematic uncertainty.

The new 18.5-GeV/c data on A have a sharp dip near $P_\perp^2=3$ (GeV/c)^2, which is similar to the dip near $P_\perp^2=3.5$ (GeV/c)^2 in the 28-GeV/c AGS data[3] and the 24-GeV/c CERN data.[10] The 12-GeV/c Argonne Zero-Gradient Synchrotron data[1] may also have a small dip near $P_\perp^2=3.5$ (GeV/c)^2. This comparison suggests that the position of this medium-$P_\perp^2$ dip in A is fairly independent of energy. Many theoretical models based on perturbative QCD suggested that all spin effects decrease at high energy and large $P_\perp^2$. The large one-spin effects recently found[3] at 28 GeV/c and $P_\perp^2=6.5$ (GeV/c)^2 disagree with the $A=0$ prediction of perturbative QCD models. Our new high-precision data show that at 18.5 GeV/c A is certainly nonzero at medium $P_\perp^2$ and is also rapidly changing.

The sharp dip in A_{nn} near $P_\perp^2=2.3$ (GeV/c)^2 seems quite interesting. Many theoretical models[11-27] have made predictions about the behavior of A_{nn}, but none has predicted this medium-$P_\perp^2$ dip at 18.5 GeV/c. At 12 GeV/c there is a sharp dip in A_{nn} near $P_\perp^2=0.9$ (GeV/c)^2 and a broad dip near $P_\perp^2=3.2$ (GeV/c)^2. It is not clear whether the sharp dip we observed at $P_\perp^2=2.3$

TABLE I. Data on A and A_{nn} at $P_{\text{lab}}=18.5$ GeV/c.

$P_\perp^2$ [(GeV/c)^2]	P_B (%)	P_T (%)	Events	A_B (%)	A_T (%)	A (%)	A_{nn} (%)
1.40	41.1	45.1	62640	13.2 ± 1.0	15.7 ± 1.9	13.8 ± 0.9	9.4 ± 2.3
1.70	41.7	45.0	79971	9.3 ± 0.9	9.4 ± 1.7	9.3 ± 0.8	11.5 ± 2.0
1.95	40.6	68.9	65687	7.7 ± 1.0	6.2 ± 0.6	6.6 ± 0.5	7.4 ± 1.5
2.25	40.7	68.5	48216	4.6 ± 1.2	3.8 ± 0.7	4.0 ± 0.6	−0.2 ± 1.7
2.45	42.5	60.6	25692	2.0 ± 1.6	−2.4 ± 1.1	−0.9 ± 0.9	−0.2 ± 2.6
2.75	42.5	60.6	21967	−0.4 ± 1.7	−2.6 ± 1.2	−1.9 ± 1.0	2.3 ± 2.8
3.05	40.4	42.6	25163	−2.1 ± 1.7	−2.0 ± 1.6	−2.0 ± 1.1	7.5 ± 3.9
3.35	40.1	42.7	12490	1.2 ± 2.4	2.1 ± 2.2	1.7 ± 1.6	13.2 ± 5.6

$(\mathrm{GeV}/c)^2$ is related to the small- or the large-$P_\perp^2$ dip at 12 GeV/c. The extension of the 18.5-GeV/c A_{nn} measurements to small $P_\perp^2$ might resolve this question. We also hope soon to extend the 18.5-GeV/c measurements to larger $P_\perp^2$ to determine if A_{nn} becomes large and positive, as at 12 GeV/c, or exhibits some other behavior. Our earlier 18.5-GeV/c measurement[5] at $P_\perp^2=4.7$ $(\mathrm{GeV}/c)^2$ with A_{nn} near zero had a rather large error as shown in Fig. 2.

Our new results at $P_{\mathrm{lab}}=18.5$ GeV/c are also plotted in Fig. 3 as the relative pure-initial-spin cross sections,

$$\sigma_{\uparrow\uparrow}\equiv\frac{d\sigma(\uparrow\uparrow)/dt}{\langle d\sigma/dt\rangle}=1+2A+A_{nn},$$
$$\sigma_{\downarrow\downarrow}\equiv\frac{d\sigma(\downarrow\downarrow)/dt}{\langle d\sigma/dt\rangle}=1-2A+A_{nn}, \quad (4)$$
$$\sigma_{\downarrow\uparrow}=\sigma_{\uparrow\downarrow}\equiv\frac{d\sigma(\uparrow\downarrow)/dt}{\langle d\sigma/dt\rangle}=1-A_{nn},$$

where $\langle d\sigma/dt\rangle$ is the spin-averaged elastic cross section. Note the rapid variations in $\sigma_{\uparrow\uparrow}$, $\sigma_{\downarrow\downarrow}$, and $\sigma_{\uparrow\downarrow}$. At our smallest $P_\perp^2$, $\sigma_{\uparrow\uparrow}$ is more than 50% larger than both $\sigma_{\downarrow\downarrow}$ and $\sigma_{\uparrow\downarrow}$. Near $P_\perp^2=2.5$ $(\mathrm{GeV}/c)^2$ all three cross sections come together and then they appear to move apart again at larger $P_\perp^2$. The 19-GeV/c spin-averaged p-p elastic-cross-section data of Allaby *et al.*[28] are also shown in Fig. 3 for comparison. Note that $\langle d\sigma/dt\rangle$ has a break and a dip near $P_\perp^2=1$ $(\mathrm{GeV}/c)^2$ followed by a second exponential which is due to hard scattering. However, $\langle d\sigma/dt\rangle$ appears to drop smoothly near the sharp structure in A and A_{nn} near $P_\perp^2=2.5$ $(\mathrm{GeV}/c)^2$. This figure suggests that the spin-averaged cross section is insensitive to large and possibly significant forces which appear quite clearly in the pure-spin cross sections.

We would like to thank the many members of the Brookhaven AGS staff who successfully operated the AGS polarized proton beam. We are grateful to Professor G. R. Court, J. M. Caraher, R. J. Garisto, and C. B. Higley for their help with the experiment. We thank the staff of the Massachusetts Institute of Technology Bates LINAC for their help with our NH_3 bead irradiation and Dr. D. A. Hill of Argonne for providing our EABA beads. This work was supported by a research contract from the U.S. Department of Energy.

[1]D. G. Crabb *et al.*, Phys. Rev. Lett. **41**, 1257 (1978); K. Abe *et al.*, Phys. Lett. **63B**, 239 (1976); J. R. O'Fallon *et al.*, Phys. Rev. Lett. **39**, 733 (1977).

[2]E. A. Crosbie *et al.*, Phys. Rev. D **23**, 600 (1981).

[3]P. R. Cameron *et al.*, Phys. Rev. D **32**, 3070 (1985); P. H. Hansen *et al.*, Phys. Rev. Lett. **50**, 802 (1983); D. C. Peaslee *et al.*, Phys. Rev. Lett. **51**, 2359 (1983).

[4]K. A. Brown *et al.*, Phys. Rev. D **31**, 3017 (1985).

[5]G. R. Court *et al.*, Phys. Rev. Lett. **57**, 507 (1986).

[6]K. M. Terwilliger *et al.*, IEEE Trans. Nucl. Sci. **32**, 2635 (1985).

[7]F. Z. Khiari *et al.*, to be published.

[8]J. A. Bywater *et al.*, unpublished.

[9]D. G. Crabb *et al.*, in *Proceedings of the Fourth International Workshop on Polarized Target Materials and Techniques, Bad Honnef, West Germany, 1984,* edited by W. Meyer (University of Bonn, Bonn, West Germany, 1984), p. 7; S. Brown *et al.*, *ibid.*, p. 66; P. R. Cameron *et al.*, *ibid.*, p. 143.

[10]J. Antille *et al.*, Nucl. Phys. **B185**, 1 (1981).

[11]G. R. Farrar, S. A. Gottlieb, D. Sivers, and G. H. Thomas, Phys. Rev. D **20**, 202 (1979); G. R. Farrar, Phys. Rev. Lett. **56**, 1643 (1986).

[12]S. J. Brodsky, C. E. Carlson, and H. J. Lipkin, Phys. Rev. D **20**, 2278 (1979).

[13]C. Bourrely, J. Soffer, and T. T. Wu, Phys. Rev. D **19**, 3249 (1979), and Nucl. Phys. **B247**, 15 (1984); C. Bourrely and J. Soffer, Phys. Rev. D **35**, 145 (1987); G. M. Preparata and J. Soffer, Phys. Lett. B **180**, 281 (1986).

[14]S. M. Troshin and N. E. Tyurin, J. Phys. (Paris), Colloq. **46**, C2-235 (1985).

[15]P. A. Kazaks and D. L. Tucker, Phys. Rev. D **37**, 222 (1988).

[16]S. J. Brodsky and G. F. de Teramond, Phys. Rev. Lett. **60**, 1924 (1988).

[17]M. Anselmino, Z. Phys. C **13**, 63 (1982); M. Anselmino and E. Leader, unpublished.

[18]H. J. Lipkin, Nature (London) **324**, 14 (1986), and Phys. Rev. Lett. B **181**, 164 (1987).

[19]A. W. Hendry, Phys. Rev. D **10**, 2300 (1974), and **23**, 2075 (1981).

[20]J. P. Ralston and B. Pire, Phys. Rev. Lett. **57**, 2330 (1986).

[21]G. R. Goldstein and M. J. Moravcsik, Phys. Rev. D **32**, 303 (1985).

[22]Y. Tomozawa, Phys. Rev. D **36**, 2854 (1987).

[23]G. F. Wolters, Phys. Rev. Lett. **45**, 776 (1980).

[24]L. Durand and F. Halzen, Nucl. Phys. **B104**, 317 (1976).

[25]M. Sakamoto and S. Wakaizumi, Prog. Theor. Phys. **62**, 1293 (1979); S. Wakaizumi, Prog. Theor. Phys. **67**, 531 (1982).

[26]C. Avilez, G. Cocho, and M. Moreno, Phys. Rev. D **24**, 634 (1981).

[27]S. V. Goloskokov, S. P. Kuleshov, and O. V. Seljugin, in *Proceedings of the Seventh International Symposium on High Energy Spin Physics, Protvino, USSR, 1986* (Institute of High Energy Physics, Serpukhov, USSR, 1987).

[28]J. V. Allaby *et al.*, Phys. Lett. **28B**, 67 (1968).

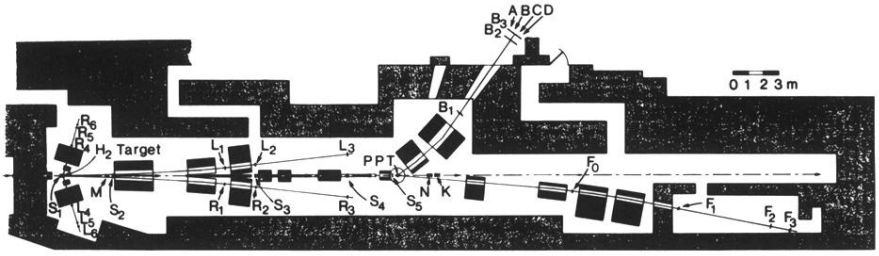

FIG. 1. Layout of the experiment. The high-energy polarimeter on the left used a liquid-hydrogen target to measure the left-right asymmetry in p-p elastic scattering. The polarized proton beam then scattered in the vertically polarized proton target and the elastic events were detected by the spectrometer which contained magnets for momentum analysis and the F and B scintillation-counter hodoscopes. The counters M, N, and K were intensity monitors, while the segmented wire ion chambers S_1, S_2, S_4, and S_5 monitored the beam's position, size, and angle.

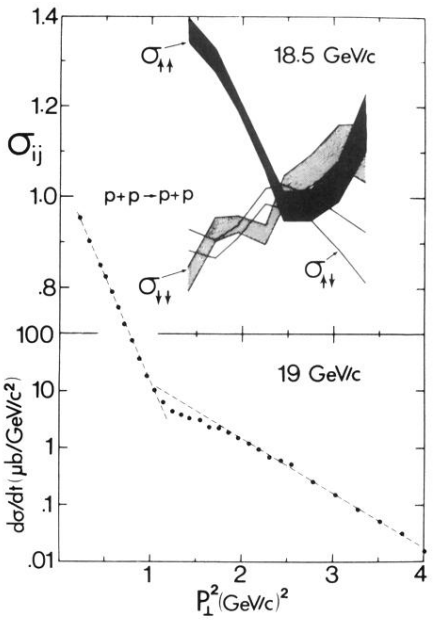

FIG. 3. The relative pure-initial-spin-state cross sections $\sigma_{\uparrow\uparrow}$, $\sigma_{\downarrow\downarrow}$, and $\sigma_{\uparrow\downarrow} \equiv [d\sigma(\uparrow\downarrow)/dt]\langle d\sigma/dt\rangle^{-1}$ plotted against $P_\perp^2$ for $p_\uparrow + p_\uparrow \rightarrow p + p$ at 18.5 GeV/c. The errors are given by the width of each band. The spin-averaged cross-section data of Allaby *et al.* (Ref. 28) at 19 GeV/c are also plotted for comparison. The dashed lines are exponentials in $P_\perp^2$.